

---

# Low-Cost On-device Partial Domain Adaptation (LoCO-PDA): Enabling efficient CNN retraining on edge devices

---

Aditya Rajagopal<sup>1</sup> Christos-Savvas Bouganis<sup>1</sup>

## Abstract

With the increased deployment of Convolutional Neural Networks (CNNs) on edge devices, the uncertainty of the observed data distribution upon deployment has led researchers to utilise large and extensive datasets such as ILSVRC'12 to train CNNs. Consequently, it is likely that the observed data distribution upon deployment is a subset of the training data distribution. In such cases, not adapting a network to the observed data distribution can cause performance degradation due to negative transfer and alleviating this is the focus of Partial Domain Adaptation (PDA). Current works targeting PDA do not focus on performing the domain adaptation on an edge device, adapting to a changing target distribution or reducing the cost of deploying the adapted network. This work proposes a novel PDA methodology that targets all of these directions and opens avenues for on-device PDA. LoCO-PDA adapts a deployed network to the observed data distribution by enabling it to be retrained on an edge device. Across subsets of the ILSVRC12 dataset, LoCO-PDA improves classification accuracy by 3.04pp on average while achieving up to 15.1x reduction in retraining memory consumption and 2.07x improvement in inference latency on the NVIDIA Jetson TX2. The work is open-sourced at [link removed for anonymity](#).

## 1. Introduction

The rapid increase in the memory and compute capability of modern edge devices has resulted in the increased deployment of CNNs on the edge. The deployment life cycle starts with the architecture and weights of the network being optimised on servers using large datasets such

as ILSVRC'12 (Krizhevsky et al., 2017). Once deployed on an edge device such as the NVIDIA Jetson TX2, networks typically remain unchanged and if adapted, require communication of data back to a server. This raises both data-privacy concerns and is not possible when there is no edge-server connectivity.

As the deployed network is trained on a large and extensive dataset such as ILSVRC'12, it is expected that the label space of the observed data distribution after deployment (target domain) is a subset of the label space of the training data distribution (source domain). However utilising this deployed network to classify solely target domain data triggers negative transfer (Cao et al., 2018). Negative transfer refers to the loss in classification performance due to the fact that the network has learnt to classify a much larger number of classes (including source-only classes) than those in the target domain. Most works in the field of Partial Domain Adaptation (PDA) aim to prevent negative transfer, but do not consider the possibility of a constantly changing target domain or the memory and compute footprint of the adaptation process or the resulting adapted network - all of which are important considerations for real-life applications.

The goal of this work is to enable the partial domain adaptation of a deployed model to be performed directly on an edge device, within some memory and time budget, to improve the performance of the adapted model on the observed target domain. Additionally, the proposed methodology is sufficiently low-cost to allow for adaptation to a changing target domain and can obtain gains in inference time memory and latency footprint by adapting a network that is smaller than that originally deployed for inference.

The novel contribution of this work is LoCO-PDA, a methodology that uses Variational Autoencoders (VAEs) to perform low-cost PDA on edge devices. As demonstrated in Fig.1, unlike other PDA methodologies, LoCO-PDA aims to optimise for the trade-off between domain adapted classification accuracy, and the adaptation process

---

<sup>\*</sup>Equal contribution <sup>1</sup>Intelligent Digital Systems Lab, Imperial College London, UK. Correspondence to: Aditya Rajagopal <adityarajagopal0@outlook.com>.

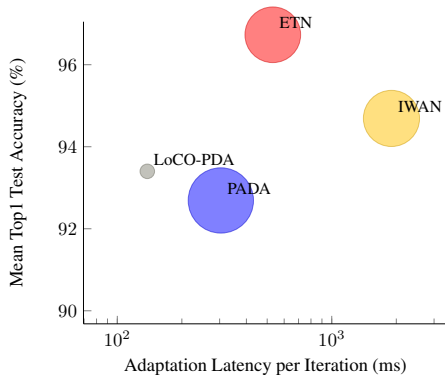


Figure 1. Adaptation process latency per iteration (x-axis), memory (dot-area) and mean accuracy (y-axis) trade-off across PDA transfer tasks on the Office31 dataset for SOTA PDA methodologies and LoCO-PDA. Please note the logarithmic x-axis.

memory consumption and latency.<sup>1</sup> It achieves on average a 7x and 4x improvement in adaptation time and memory respectively while performing comparably to other SOTA PDA methodologies.

## 2. Background and Related Works

### 2.1. Partial Domain Adaptation (PDA)

As discussed in (Cao et al., 2019), the primary focus of unsupervised domain adaptation is on learning domain-invariant feature representations without access to target domain labels, so that the same feature extractor and classifier combination can be utilised in both the source and target domains. However, these works (Saenko et al., 2010; Gong et al., 2012) assume that both source and target domains have the same label space, which is an unlikely scenario to be observed in reality. A more likely scenario in real-world deployments is PDA where the target label space is assumed to subsume the source label space.

The challenge addressed by SOTA works targeting PDA such as ETN (Cao et al., 2019), IWAN (Zhang et al., 2018), and PADA (Cao et al., 2018) is to train a feature extractor that generates an aligned activation distribution for classes of images that are common to both source and target domains, while preventing distribution alignment on source only classes. All three works utilise an adversarial framework that consists of a feature extractor and domain classifier. The domain classifier aims to identify in an unsupervised manner the difference between the source and target domains, while the feature extractor is trained to reduce the discrepancy between the domains. The domain classifier outputs weights that identify classes as source-only or shared; and the three works vary in their approaches to util-

<sup>1</sup>Times are collected on the server grade NVIDIA 2080Ti as SOTA methodologies are too memory intensive to be run on the Jetson TX2 edge device.

ising these weights in training the feature extractor.

Different to such approaches, this work proposes a novel solution to the problem of PDA which does not change the source domain feature extractor but rather retrains just the classifier to better discriminate between the classes observed in the target domain. We propose to estimate the target domain label subspace using predictions of the deployed model. As no ground-truth labels are used, this approach is still unsupervised. Furthermore, compared to adversarial PDA approaches, the proposed methodology has a low enough memory and compute requirement to be performed directly on an edge device and benefits from adaptability to changes in the target domain.

### 2.2. Edge Device CNN Training

To the best of our knowledge, the only two works which also explore on-device training of CNNs are TinyTL (Cai et al., 2020b) and PersEPhonEE (Leontiadis et al., 2021). TinyTL proposes a variation of the MBConv (Sandler et al., 2018) layer called a Lite-Residual layer which downsamples the input activations, performs grouped and 1x1 convolutions on them, upsamples the output and adds it to the output of the original MBConv layer. By only retraining the *lite* bypass layers on the edge, the methodology reduces memory requirements of training as only downsampled intermediate activations need to be stored. TinyTL is evaluated on a transfer-learning scenario where the source and target domains do not share the same label space and there is access to ground-truth labels of the target domain. This is outside the scope of this work and hence is not compared to.

PersEPhonEE proposes an early-exit methodology instead of pruning to reduce the cost of both inference and training on an edge device. By placing an early exit after various residual blocks along ResNet50, the authors propose to improve both training and inference time by only retraining the desired early-exit block. They demonstrate between 2x-22x improvement in training latency depending on the early-exit used and up to 20pp improvement in classification accuracy depending on the target domain. The authors provide results for various subsets of the ILSVRC’12 dataset and propose to use the output of the final classifier as labels to retrain earlier classifiers (unsupervised). Thus this work falls under the PDA framework and is compared against.

## 3. Problem Description

The inputs to the system are a model  $\mathcal{M}^0$  and a large training data distribution  $\mathcal{D}$ . Let  $\mathcal{M}^0$  be the model that has been trained on  $\mathcal{D}$  and prepared for initial deployment on an edge device. Upon deployment, the system observes a data dis-

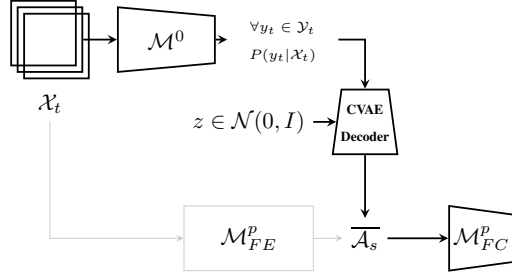


Figure 2. Proposed methodology for low-cost adaptation of the pruned network’s classifier ( $\mathcal{M}_{FC}^p$ ).  $\mathcal{M}^0$  produces a set of predicted labels ( $\mathcal{Y}_t$ ), for target domain images  $\mathcal{X}_t$ . The predicted classes along with their frequency of occurrence ( $P(y_t|\mathcal{X}_t)$ ) is provided to the trained decoder. The decoder then generates a set of estimated activations  $\bar{\mathcal{A}}_s$  which can be used to train the pruned network’s classifier. Consequently, this process bypasses the feature extractor of the pruned network ( $\mathcal{M}_{FE}^p$ ).

tribution  $\mathcal{D}'$  that is assumed to be able to change over time. Furthermore, the label space of  $\mathcal{D}'$  is assumed to be a subset of that of  $\mathcal{D}$ . Due to this assumption, it is expected that a model ( $\mathcal{M}^p$ ), that has a lower memory and latency footprint than  $\mathcal{M}^0$  can be adapted to the observed  $\mathcal{D}'$  after deployment as a smaller number of classes are being classified ( $\mathcal{D}' \subset \mathcal{D}$ ). This results in an adapted network that has significant gains in inference memory and latency. In this work we consider  $\mathcal{M}^p$  to be a network that is obtained by pruning away  $p\%$  of the memory footprint of  $\mathcal{M}^0$ .<sup>2</sup> However, LoCO-PDA can be applied even if  $\mathcal{M}^0$  and  $\mathcal{M}^p$  are completely different networks.

The goal and novel contribution of this work is to create a system that enables the retraining of  $\mathcal{M}^p$  on an edge device such that the accuracy of  $\mathcal{M}^p$  on  $\mathcal{D}'$  is at least as good as that of  $\mathcal{M}^0$  on  $\mathcal{D}'$ .

## 4. Low-cost Training

This section motivates the proposed training methodology by identifying methods to reduce the cost of retraining. The greyed out path in Fig.2 is an abstraction of a CNN network architecture. The feature extractor ( $\mathcal{M}_{FE}^p$ ) takes as input an image and outputs activations that are then passed to the classifier ( $\mathcal{M}_{FC}^p$ ) to predict the class of the image. The cost of training the feature extractor is significantly larger than that of the classifier. As stated in (Cai et al., 2020b), the limiting factor of training CNNs on edge devices is the memory required to store intermediate activations used by backpropagation. Consequently, the primary cost of retraining a CNN lies in the feature extractor stage and bypassing this would significantly reduce the cost of retraining a network.

<sup>2</sup>The pruning and retraining process is performed offline on  $\mathcal{D}$ . Both Taylor First Order (TFO) (Molchanov et al., 2019) and OFA (Cai et al., 2020a) methodologies are used for pruning.

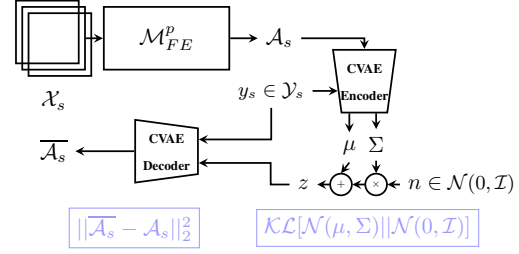


Figure 3. VAE training process used to train the decoder that is used in Fig.2. The whole process is performed offline using source domain images ( $\mathcal{X}_s$ ) and available ground truth source domain labels ( $\mathcal{Y}_s$ ). The CVAEs are trained to reproduce source domain activations ( $\mathcal{A}_s$ ) when provided with the desired class  $y_s$  and a random vector  $z$  sampled from a multivariate standard normal distribution. The blue boxes show the loss functions used to train the CVAEs, where the left box is the reconstruction mean-squared-error (MSE) between the estimated activations  $\bar{\mathcal{A}}_s$  and the true activations  $\mathcal{A}_s$  and the right box is the KL-divergence between the learnt distribution of the latent space ( $\mathcal{N}(\mu, \Sigma)$ ) and  $\mathcal{N}(0, \mathcal{I})$ .

One way to bypass the training of the feature extractor stage is to only train the classifier. This only requires inference, which is a highly optimised process on edge devices. However, doing so also requires the storage of images with which retraining can be performed. This can be infeasible on edge devices due to the limited available memory. Consequently, LoCO-PDA aims to retrain just the classifier but also bypass the execution of the feature extractor, thereby significantly reducing the memory requirements of the retraining process.

## 5. Methodology

Most modern networks have linear classifier layers as they have highly expressive feature extractors that create representations of images (activations) that can be linearly separated. LoCO-PDA exploits the simplicity of these activations and uses light-weight VAEs to generate them instead of performing inference through the feature extractor of  $\mathcal{M}^p$ . These generated activations can then be used to train the classifier. This process is described by the black path in Fig.2. Utilising a pruned model achieves gains in inference memory consumption and latency, while retraining the classifier allows the pruned network to regain the accuracy lost by pruning while also optimising the network’s weights to the observed data distribution. There is no added overhead to performing inference through  $\mathcal{M}^0$  as this is the originally deployed model which is being used for inference and thus statistics of  $P(y_t|\mathcal{X}_t)$  can be collected over time before initiating retraining.

### 5.1. VAE Training Process

LoCO-PDA uses an extension of VAEs known as Conditional-VAEs (CVAEs). VAEs (Kingma and Welling,

2014) are generative models that learn to model some distribution  $P(t)$  where  $t$  are high-dimensional data points which can represent a variety of inputs. They do this by learning a latent representation that can then be sampled to generate data points close  $P(t)$ . Fig.3 shows the process of training the CVAEs to generate the activations of  $\mathcal{M}^p$  at the output of the feature extractor. CVAEs (Sohn et al., 2015) allow for the sampling of the latent space to be conditioned on a desired class of  $\mathcal{A}_s$ . One CVAE is required per source domain dataset  $\mathcal{D}$  and model  $\mathcal{M}^p$  and they are trained on  $\mathcal{M}^p$ 's activations for all images ( $\mathcal{X}_s$ ) in  $\mathcal{D}$  before deployment.

The encoder in Fig.3 learns the function  $q_\phi(z|\mathcal{A}_s, y_s)$  which maps activations to latent space variables. The decoder then learns the function  $p_\theta(\mathcal{A}_s|z, y_s)$  which generates an activation corresponding to provided class. It learns to generate activations for all source domain classes ( $\mathcal{Y}_s$ ) in order to be able to adapt to varying target domains.

The loss function used is that proposed in (Higgins et al., 2017) for conditional VAEs and is given by:

$$\mathcal{L}(\theta, \phi; \mathcal{A}_s, z, y_s, \beta) = \mathbb{E}_{q_\phi(z|\mathcal{A}_s, y_s)} [\log p_\theta(\mathcal{A}_s|z, y_s)] - \beta \mathcal{KL}(q_\phi(z|\mathcal{A}_s, y_s) || p(z)) \quad (1)$$

The weights of the encoder and decoder that are learnt are given by  $\phi$  and  $\theta$  respectively.  $\beta$  is a parameter that balances the trade-off between reconstruction error and latent space regularisation.  $p(z)$  is the prior distribution and is set to  $\mathcal{N}(\mathbf{0}, \mathbf{I})$  in order to obtain a closed form solution to the regularisation term. The conditional decoding process samples  $z \sim \mathcal{N}(\mathbf{0}, \mathbf{I})$ , augments the variable with  $y_s$  corresponding to the desired class and provides this as input to the trained decoder as shown in Fig.2. This process is facilitated by learning a latent space that closely follows  $\mathcal{N}(\mathbf{0}, \mathbf{I})$  (KL-divergence loss term), thus training a decoder that can map a randomly sampled variable in this distribution to the desired network activation based on the conditioning information.<sup>3</sup>

## 5.2. Identifying $\mathcal{D}'$

Once the VAE is trained, it is deployed along with the initial deployment model  $\mathcal{M}^0$  and the pruned model  $\mathcal{M}^p$  that will be adapted to the observed data distribution. Before retraining  $\mathcal{M}^p$  on  $\mathcal{D}'$ , it is necessary to identify the labels observed. We propose to identify these labels from the distribution predicted by the currently deployed network  $\mathcal{M}^0$  (Fig.2). The assumption here is that  $\mathcal{M}^0$  has sufficient accuracy to identify the classes observed upon deployment.

<sup>3</sup>Refer to Appendix A.1 for the training hyperparameters.

## 5.3. Retraining $\mathcal{M}^p$

The retraining process gets as input a distribution  $P(y_t|\mathcal{X}_t)$  which assigns a probability per observed class based on the frequency with which that class was observed. The tunable parameter  $R$  decides how many total activations to use when performing the classifier retraining. The  $R$  activations that are generated follow the class distribution  $P(y_t|\mathcal{X}_t)$ , thus a sufficiently small probability could result in no activation being generated for that class. Under the assumption that  $\mathcal{M}^0$  predicts the correct class with a sufficiently high probability, this approach can be robust to noisy class distributions generated by  $\mathcal{M}^0$  that may contain incorrect class predictions. These activations are then used to train  $\mathcal{M}^p$ 's classifier. Compared to the feature extractor, the decoder can be up to 20x smaller in terms of memory footprint which reduces the cost of retraining such that it can be performed on a CPU within a reasonable time budget.<sup>4</sup>

## 6. Evaluation

This section first evaluates LoCO-PDA under the constraints of a practical deployment scenario. Sec.6.7 then compares LoCO-PDA to other SOTA PDA methodologies.

Consider the following scenario, as proposed by (Rajagopal and Bouganis, 2021), of an autonomous vehicle running an image classification CNN on an NVIDIA Jetson TX2 edge device. As the environment the car observes varies over time, the weights of a pruned version of the deployed CNN can be adapted to specialise this network to the data observed. The Jetson TX2 has only 8GB of memory that is shared between the CPU and GPU. Apart from the image classification network, there are other safety critical applications running on the device.

This scenario introduces the following considerations. As the device has a unified memory system, memory intensive processes such as retraining started on either processor can affect processes from executing on the other. In safety critical scenarios, this could have catastrophic consequences. On-device retraining of CNNs is primarily limited by its memory consumption and for many CNNs even batch sizes as low as 32 requires too much memory. Additionally, the robustness of the methodology to the lack of ground-truth labels of the observed data is an important consideration.

Consequently all approaches in this section are evaluated on the following metrics. Static (storage) and runtime memory consumption. Classification accuracy of the adapted network on  $\mathcal{D}'$ . Performance under noisy  $\mathcal{D}'$  estimation. Wall-clock time to perform on-device adaptation on both the GPU and CPU. Inference latency and total floating-

<sup>4</sup>Refer to Appendix A.2 for the retraining hyperparameters

point operations (FLOPs) of the adapted network.

### 6.1. Evaluation Datasets and Methodologies

This section details the methodologies that will be evaluated and the datasets that they will be evaluated on. For all experiments in this section, the training hyperparameters provided in Appendix A.1 and A.3 were used.

#### 6.1.1. DATASETS

For all experiments in this section, the source domain dataset ( $\mathcal{D}$ ) on which model training and pruning are performed is the entire ILSVRC'12 training set.

For the practical deployment scenario, adaptation to four example target domain datasets ( $\mathcal{D}'$ ) will be explored. These are constructed as subsets of the ImageNet dataset that emulate different environments that an autonomous vehicle could encounter (Rajagopal and Bouganis, 2021). They are City (185 classes), Motorway (26 classes), Country-side (204 classes), Off-road (26 classes). Furthermore, for this evaluation, an edge-retraining dataset is created by randomly sampling 20% of the ImageNet training dataset. For each  $\mathcal{D}'$ , images from this dataset are utilised to emulate images that a deployed network would classify and are used to retrain the network on the edge. Although the deployed network has already observed these images during training on ImageNet, a different random seed is used for image preprocessing and augmentation to emulate variation from the training distribution. Doing so allows for all accuracy results to be reported on the full ImageNet validation dataset (unseen by models) to allow for fair comparison in the future.

When evaluating the methodology against other resource unconstrained PDA approaches, the Caltech-84 and Office-31 datasets are used. The Caltech-84 dataset uses the 84 classes that are shared between the ILSVRC'12 and Caltech-256 (Griffin et al., 2006) datasets. The Office-31 dataset consists of 3 categories corresponding to images from *Amazon*, a *DSLR* and a *Webcam* and each category has images corresponding to 31 classes. These target domains are common transfer learning benchmarks and details of the classes present in all target domains are provided in Appendix D.

#### 6.1.2. METHODOLOGIES

The methodologies that LoCO-PDA is compared against under the practical deployment scenario setting store a set of  $N$  possible pruned models on-device, each of which can be retrained to the observed data distribution. The choice of model that is retrained depends on the target inference memory and latency at the time of deployment. The methodologies vary in either pruning strategy or the man-

ner in which multiple networks with different budgets are exposed.

**On-device Retraining** A set of  $N$  pruned models are obtained using both Taylor First Order (Molchanov et al., 2019) and OFA pruning (Cai et al., 2020a). All pruning is performed using the tool open sourced in (Rajagopal and Bouganis, 2020). For both pruning strategies, on device retraining on  $\mathcal{D}'$  of all-layers and classifier-only are considered as baselines.

**PersEPhonEE** This methodology appends early-exit modules which contain two convolution layers and a classifier at various points along the backbone network. After training of all exits and the backbone network offline on  $\mathcal{D}$ , on-device retraining cost is minimised by only finetuning the early exit that falls within the available memory and compute budget.

To the best of our knowledge, PersEPhonEE is the only other work that explores edge device retraining for PDA. The TFO and OFA approaches are baselines to evaluate the robustness of LoCO-PDA to different pruning strategies.

For all methodologies, both memory bounded and unbounded training approaches are evaluated. This refers to placing a memory limit on the number of images that can be stored in order to perform retraining versus utilising the entire retraining dataset which as discussed in Sec.6.1.1 corresponds to 20% of the ILSVRC'12 training dataset. In the memory bounded scenario, a limit of 400MB is set as this is deemed to be a reasonable allocation of the available 8GB on a Jetson TX2 for this purpose. In the memory unbounded scenario, as each  $\mathcal{D}'$  has a different number of classes, the storage memory utilised varies and is 9.40 GB, 1.36 GB, 10.3 GB and 1.36 GB for the City, Motorway, Country-side, and Off-road  $\mathcal{D}'$  respectively. The memory unbounded scenario evaluates the best case performance of each methodology when not subjected to any memory constraints. All retraining based approaches are evaluated on the NVIDIA Jetson TX2 using PyTorch v1.6, CUDA 10.2, cuDNN 8.0 and batch-size 32. Under the scenario where ground-truth labels in the target domain are used, these methodologies act as an "oracle" for retraining a network directly on the target domain.

For resource unconstrained PDA, LoCO-PDA is compared against ETN (Cao et al., 2019), IWAN (Zhang et al., 2018) and PADA (Cao et al., 2018).

#### 6.1.3. NETWORKS

The  $\mathcal{M}^0$  and  $\mathcal{M}^p$  networks utilised in this evaluation are shown in Table.1. As discussed in Sec.6.1.2,  $N$   $\mathcal{M}^p$  networks are stored on device, however for simplicity this section only evaluates the case of  $N = 1$ .

Table 1. Summary of inference operations (OPS), Model memory footprint (MODEL), Jetson TX2 single image inference latency (LAT) and ILSVRC’12 Test Top1 accuracy (ACC)

		OPS (MFLOPS)	MODEL (MB)	LAT (ms)	ACC (%)
<b>TFO</b>	$\mathcal{M}_{TFO}^0$	4087	102	45.13	76.12
	$\mathcal{M}_{TFO}^{80}$	1250	41	36.66	63.74
<b>OFA</b>	$\mathcal{M}_{OFA}^0$	3496	126	42.34	83.89
	$\mathcal{M}_{OFA}^{80}$	1197	40	20.44	81.75
<b>PERSPHONEE</b>	$\mathcal{M}_{PE}^0$	4087	143	45.13	76.12
	$\mathcal{M}_{PE}^{80}$	1246	143	16.65	16.91

Table 2. Static and runtime memory consumption of the various methodologies. NETWORK refers to the model storage requirements. IMAGES refers to the storage of images for retraining.

		STATIC (MB)		RUNTIME (MB)	TOTAL (MB)
		NETWORK	IMAGES		
<b>TFO</b>	Classifier-only	143	400	1668	2211
	All-Layers			3508	4052
	<b>LoCO-PDA (CPU)</b>			13	<b>166</b>
	LoCO-PDA (GPU)	153	0	1143	1296
<b>OFA</b>	Classifier-only	166	400	1865	2431
	All-Layers			2800	3366
	<b>LoCO-PDA (CPU)</b>			28	<b>277</b>
	LoCO-PDA (GPU)	249	0	1128	1337
<b>PERSPHONEE</b>		143	400	1971	2513

$\mathcal{M}_{TFO}^0$  is an unpruned ResNet50 network and  $\mathcal{M}_{TFO}^{80}$  is the same network TFO pruned by 80%.  $\mathcal{M}_{OFA}^0$  is the largest sub-network that can be sampled from the OFA super network and  $\mathcal{M}_{OFA}^{80}$  is an OFA sub-network that has a similar FLOPs budget to  $\mathcal{M}_{TFO}^{80}$ .  $\mathcal{M}_{PE}^0$  is an unpruned ResNet50 network augmented with 6 early exits located at FLOPs normalised locations along the network. Consequently, apart from *model memory*, all other metrics are the same as  $\mathcal{M}_{TFO}^0$  in Table.1.  $\mathcal{M}_{PE}^{80}$  is the second early exit (after layer2.1) as this has a similar FLOPs budget to  $\mathcal{M}_{TFO}^{80}$ .<sup>5</sup>

## 6.2. Static and Runtime Memory Footprint

Static memory footprint of a methodology corresponds to the storage memory consumed by the various parts of the methodology required to perform network adaptation. Runtime memory footprint corresponds to the memory consumed during network adaptation. Note that this is the footprint of the network adaptation process and not that of performing inference on the network. The total static and runtime memory consumption of the various methodologies on a Jetson TX2 is displayed in Table.2.

**TFO, OFA: Image based retraining** For each methodology (TFO, OFA), the static network storage component consists of the corresponding  $\mathcal{M}^0$  to estimate labels and

<sup>5</sup>Refer to Appendix B for results on other architectures.

Table 3. Best achieved Top1-Test accuracy for the various base-line approaches to on-device retraining. Values are averaged over all four autonomous driving  $\mathcal{D}'$ .

	ALL LAYERS		CLASSIFIER ONLY		
	$\mathcal{M}_{TFO}^{80}$	$\mathcal{M}_{OFA}^{80}$	$\mathcal{M}_{TFO}^{80}$	$\mathcal{M}_{OFA}^{80}$	$\mathcal{M}_{PE}^{80}$
<b>MEMORY BOUNDED</b>	76.88	81.44	75.15	82.83	23.79
<b>MEMORY UNBOUNDED</b>	81.19	83.14	79.22	84.63	26.70

$\mathcal{M}^{80}$  which is adapted through retraining. Note depending on the number ( $N$ ) of pruned networks ( $\mathcal{M}^p$ ) stored, the static network storage component will increase. Here, the case of  $N = 1$  is evaluated. The static image storage component consists of 400MB of images for memory bounded retraining. The runtime memory consumption is affected by whether classifier-only or all-layer retraining is performed and is quoted for retraining  $\mathcal{M}^{80}$  on the GPU of the Jetson TX2.

**PersEPhonEE: Early-exit retraining** The network component of the static memory consumption is from  $\mathcal{M}_{PE}^{80}$ . The images component of the static memory consumption is from the 400 MB of images stored to perform memory bounded early-exit retraining. The runtime component is from performing on-device retraining of the second early exit (Sec.6.1.3) on the GPU.

**LoCO-PDA** For LoCO-PDA, the additional static network component is storage of the CVAE model used to generate activations. This component is 9.65 MB for  $\mathcal{M}_{TFO}^{80}$  and 16.83 MB for  $\mathcal{M}_{OFA}^{80}$ . As PersEPhonEE uses  $\mathcal{M}_{TFO}^0$  as the backbone network, the CVAE trained on activations generated by  $\mathcal{M}_{TFO}^{80}$  is used for comparison. No images are used for retraining with this approach, hence the static image component is 0 MB. The memory consumed by the generated activations is incorporated into the runtime memory consumption which is evaluated both on the CPU and GPU of the Jetson TX2. The significantly extra memory consumption of the GPU is due to CUDA initialisation overheads which can be close to 1 GB depending on the device and framework combination. LoCO-PDA executed on a CPU consumes 13.3x, 8.76x and 15.1x less memory compared to TFO classifier-only retraining, OFA classifier-only retraining and second exit training of PersEPhonEE respectively executed on a GPU.

## 6.3. Accuracy of $\mathcal{M}^p$ on $\mathcal{D}'$

This section compares the best achieved Top1-Test accuracy after adapting the network to the four autonomous driving  $\mathcal{D}'$ s for all the methodologies discussed in Sec.6.1.2. In order to evaluate the methodologies under a no-uncertainty situation, all results here assume knowledge of the ground-truth labels for the images in  $\mathcal{D}'$ . Later sec-

tions evaluate the effect of uncertain labels when using  $\mathcal{M}^0$  to identify  $\mathcal{D}'$ . First, memory bounded and unbounded; and all-layers and classifier-only training approaches are evaluated.

### 6.3.1. MEMORY BOUNDED VS. UNBOUNDED

As seen in Table 3, the memory unbounded approach outperforms the memory bounded approach by 2.64pp on average across  $\mathcal{D}'$  and methods. Given the small performance difference (2.64pp) and the large memory requirements (3.4x) of the memory unbounded approach vs. the memory bounded approach, the rest of the evaluation focuses on the memory bounded case.

### 6.3.2. ALL LAYERS VS. CLASSIFIER-ONLY

Retraining all layers performs on average across  $\mathcal{D}'$  0.2pp worse than classifier-only training. Furthermore, retraining all layers has a runtime memory footprint that is 1.8x and training latency that is 3.4x larger than classifier-only training. Hence the following sections use classifier-only retraining as a baseline.

### 6.3.3. LOCO-PDA

The *No Label Space Uncertainty* columns of Table.4 display the achieved Test Top1 accuracy on each autonomous driving  $\mathcal{D}'$  for  $\mathcal{M}_{TFO}^{80}$  and  $\mathcal{M}_{OFA}^{80}$  when *no retraining*, *memory bounded classifier-only retraining* and *LoCO-PDA* are performed on-device. PersEPhonEE was not compared against here due to its poor performance (Table.3). This poor performance is due to utilising predictions from an early exit placed only after the second Bottleneck block of ResNet50 to allow for a FLOPs normalised comparison between methodologies (6.1.3).

The following results are averages across both the OFA and TFO networks. LoCO-PDA consistently outperforms memory bounded retraining of  $\mathcal{M}^{80}$  by 1.46pp on average across all  $\mathcal{D}'$ . Furthermore, on the smaller  $\mathcal{D}'$  (Motorway, Off-road), on which domain adaptation is more beneficial, LoCO-PDA also outperforms its corresponding unpruned network ( $\mathcal{M}^0$ ) by 3.04pp on average. Intuitively, larger subsets do not benefit significantly from on-device adaptation as the initial network optimised on many classes learns a classifier that best separates a space with many classes.

## 6.4. Storage Memory Limitations

The results from the previous sections utilise a storage memory limit of 400MB for image based retraining approaches. However, as discussed in Sec.6.3.1 placing this restriction did have a reduction in accuracy when compared to the memory unbounded scenario. This section expands on this to demonstrate the effect of various storage limits

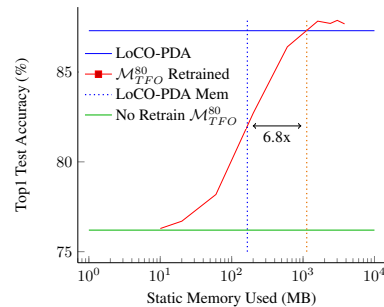


Figure 4. Effect of available image storage memory on achieved retraining accuracy for the Off-road  $\mathcal{D}'$ . Please note the logarithmic scale on the x-axis.

on the achieved accuracy when performing image based classifier-only retraining. The red line in Fig.4 displays the achieved classifier-only retraining accuracy for  $\mathcal{M}_{TFO}^{80}$  on the Off-road  $\mathcal{D}'$  as the available memory to store images is varied (x-axis). These values are the average of five retraining runs. The solid green line displays the no retraining accuracy of  $\mathcal{M}_{TFO}^{80}$  and the solid blue line displays the accuracy achieved by LoCO-PDA. The dashed blue line is the static memory consumed by LoCO-PDA. The graphs show that as the available memory budget is increased, the achieved retraining accuracy improves and depending on  $\mathcal{D}'$  can outperform LoCO-PDA under no label uncertainty while utilising 6.8x times the memory. For the same memory budget as LoCO-PDA, the memory-bounded retraining approach performs on average 4.88pp worse than LoCO-PDA.

## 6.5. Noisy $\mathcal{D}'$ Estimation

All results presented thus far assume knowledge of the label space of  $\mathcal{D}'$  which is not representative of real deployment scenarios. In this work we propose to estimate the label space of  $\mathcal{D}'$  using the predictions of the initially deployed model  $\mathcal{M}^0$ . As the accuracy of this model is not 100%, some of the labels obtained from this model are incorrect. This section evaluates the effect on achieved adaptation accuracy of noisy  $\mathcal{D}'$  estimation. The following results are averages across both the OFA and TFO networks.

The *Label Space Uncertainty* columns in Table.4 show the achieved test top1 accuracy on  $\mathcal{D}'$  for both the memory bounded classifier-only retraining strategy (RETRAINED) and the LoCO-PDA approach. For the image based retraining approaches, memory bounded retraining with uncertain labels causes a 7.27pp degradation in achieved accuracy compared to retraining with certain labels across  $\mathcal{D}'$ . Furthermore in most cases, retraining with noisy labels actually degrades the network’s accuracy compared to  $\mathcal{M}^{80}$  without any retraining. On the other hand, LoCO-PDA only incurs a 0.67pp reduction in achieved accuracy across  $\mathcal{D}'$  and never a degradation compared to  $\mathcal{M}^{80}$  without retrain-

Table 4. On-device domain adaptation accuracy of  $\mathcal{M}_{TFO}^{80}$  and  $\mathcal{M}_{OFA}^{80}$ . RETRAINED is the 400MB memory bounded, classifier-only retraining strategy. The number of classes in each  $\mathcal{D}'$  is provided in brackets. Results show label space certain and uncertain scenarios.

	$\mathcal{M}_{TFO}^{80}$ (%)		$\mathcal{M}_{OFA}^{80}$ (%)		NO LABEL SPACE UNCERTAINTY						LABEL SPACE UNCERTAINTY				
	NO RETRAIN	NO RETRAIN	NO RETRAIN	RETRAINED	LoCO-PDA	NO RETRAIN	RETRAINED	LoCO-PDA	RETRAINED	LoCO-PDA	RETRAINED	LoCO-PDA	RETRAINED	LoCO-PDA	
CITY (185)	78.01	81.64	70.89	71.11	73.84	78.50	80.37	80.73	66.36	72.33	76.59	80.67			
MOTORWAY (26)	74.54	78.28	68.23	71.28	76.75	74.85	79.91	79.86	53.93	75.20	73.49	79.05			
COUNTRY-SIDE (204)	78.48	81.98	71.36	71.78	74.03	79.07	80.28	81.22	67.82	73.04	78.12	80.56			
OFF-ROAD (26)	82.87	85.99	76.20	86.43	87.30	82.32	90.78	89.94	72.13	86.88	85.38	90.55			

Table 5. The on-device network adaptation time for various methodologies averaged across  $\mathcal{D}'$ . The quoted time in min:sec is the time taken to achieve the accuracy provided in Table.4.

	TFO		OFA	
	RETRAINED	LoCO-PDA	RETRAINED	LoCO-PDA
GPU (MIN:SEC)	02:43	00:12	02:02	00:10
CPU (MIN:SEC)	329:53	00:46	344:00	00:54

ing.

With image based retraining, predicting an incorrect label and utilising this combination to retrain the network causes increased confusion as the network is now being trained to associate incorrect labels and images. As LoCO-PDA generates the activations corresponding to the estimated class, only an incorrect ratio of the labels is generated and the retraining stage still associates labels with their correct corresponding activations. Thus, LoCO-PDA is significantly more robust to noisy estimations of  $\mathcal{D}'$  than image based retraining approaches.

## 6.6. On-device Adaptation Wall-clock Time

This section evaluates the wall-clock time to perform on-device adaptation using each methodology on the Jetson TX2. The values in Table.5 are the time taken to retrain the pruned network until the accuracy under the *No Label Space Uncertainty* case in Table.4 is achieved. As different  $\mathcal{D}'$  behave differently under retraining, the quoted values are averaged across the four  $\mathcal{D}'$ . The time taken to perform on-device adaptation for image based retraining approaches is infeasible on a CPU, hence the GPU times are utilised here for comparison. The results show that LoCO-PDA executed on a CPU and GPU outperform classifier-only retraining on a GPU by 2.9x and 12.9x respectively.

By bringing domain adaptation latencies down to less than a minute, while consuming less than 300 MB of memory and being significantly robust to noisy estimations in  $\mathcal{D}'$ , LoCO-PDA opens up avenues for on-device partial domain adaptation of networks that have not been explored before.

## 6.7. Partial Domain Adaptation

This section compares LoCO-PDA against SOTA PDA methodologies ETN (Cao et al., 2019), IWAN (Zhang et al., 2018), and PADA (Cao et al., 2018). As

Table 6. Comparison of LoCO-PDA to SOTA PDA approaches. The domains are Caltech-84 (C84), Amazon (A), DSLR (D) and Webcam (W). The ResNet50 column corresponds to a ResNet50 network trained on the source domain without further adaptation.

	RESNET50	SOTA			LoCO-PDA
		ETN	IWAN	PADA	
ILSVRC'12 → C84	69.69	83.23	78.06	75.03	79.17
A → W	76.03	94.52	89.15	86.54	84.64
A → D	91.12	95.03	90.45	82.17	90.56
OFFICE31					
D → W	94.06	100.0	99.32	99.32	97.50
D → A	83.62	96.21	95.62	92.69	93.74
W → A	88.42	94.64	94.26	95.41	93.95
W → D	98.69	100.0	99.36	100.0	100.0

these works do not consider the case of pruning a network, the reported results in this section are for an unpruned ResNet50.

For the ILSVRC'12 to Caltech-84 transfer setting, activations corresponding to the 84 classes shared between the ILSVRC'12 and Caltech-256 datasets are generated using a CVAE trained on ILSVRC'12 data that has no knowledge of the target Caltech-84 activation distribution. Furthermore, the target distribution is estimated using the output of classifying the entire Caltech-84 dataset on the unpruned ResNet50 network, hence no ground-truth labels were used. For the Office-31 setting, ResNet50 is first finetuned to each of the three categories using all 31 classes and 3 CVAEs are trained to generate activations for each of these source domain networks. The target domain images are then classified on the source domain finetuned network to obtain a distribution and the corresponding CVAE is used to generate activations to retrain the network.

On average across all PDA settings, Table.6 shows that LoCO-PDA improves performance compared to no domain adaptation and PADA by 5.42pp and 1.20pp respectively; and performs comparably to IWAN (only 0.95pp worse). Although performing 3.43pp worse compared to ETN, LoCO-PDA has the significant advantage over all three methodologies that it can rapidly adapt to changes in the target domain. PADA, IWAN and ETN cannot be performed on an edge device to re-adapt a network to new domains due to their large memory and latency footprints (Fig.1).

## 7. Conclusion

This work proposes LoCO-PDA, a methodology to perform low cost on-device partial domain adaptation of CNNs along with an open-sourced implementation. In the case where a pruned version of a network is adapted to the observed target domain, the proposed methodology achieves up to 3.27x reduction in model memory footprint and 2.07x improvement in inference latency while achieving on average 3.04pp improvement in classification accuracy compared to an unpruned version of the network that is deployed without any domain adaptation. Compared to other image based on-device retraining methodologies, LoCO-PDA achieves up to 15.1x runtime memory consumption improvements while also being significantly more robust to noisy estimations of the target domain class distribution. The entire retraining process can be performed on a CPU with sub-minute domain adaptation times on a Jetson TX2 device, opening avenues for on-device PDA which have not been explored before. LoCO-PDA also performs comparably to other SOTA PDA methodologies while benefiting from the ability to adapt to varying target domains, which the other methodologies cannot.

## References

- Bowman, S. R., Vilnis, L., Vinyals, O., Dai, A. M., Józefowicz, R., and Bengio, S. (2015). Generating sentences from a continuous space. *CoRR*, abs/1511.06349.
- Cai, H., Gan, C., Wang, T., Zhang, Z., and Han, S. (2020a). Once for all: Train one network and specialize it for efficient deployment. In *International Conference on Learning Representations*.
- Cai, H., Gan, C., Zhu, L., and Han, S. (2020b). Tiny transfer learning: Towards memory-efficient on-device learning. *CoRR*, abs/2007.11622.
- Cao, Z., Ma, L., Long, M., and Wang, J. (2018). Partial adversarial domain adaptation. *CoRR*, abs/1808.04205.
- Cao, Z., You, K., Long, M., Wang, J., and Yang, Q. (2019). Learning to transfer examples for partial domain adaptation. *CoRR*, abs/1903.12230.
- Gong, B., Shi, Y., Sha, F., and Grauman, K. (2012). Geodesic flow kernel for unsupervised domain adaptation. In *2012 IEEE Conference on Computer Vision and Pattern Recognition*, pages 2066–2073.
- Griffin, G., Holub, A., and Perona, P. (2006). Caltech256 image dataset.
- Higgins, I., Matthey, L., Pal, A., Burgess, C. P., Glorot, X., Botvinick, M., Mohamed, S., and Lerchner, A. (2017). beta-vae: Learning basic visual concepts with a constrained variational framework. In *ICLR*.
- Kingma, D. P. and Ba, J. (2015). Adam: A method for stochastic optimization. *CoRR*, abs/1412.6980.
- Kingma, D. P. and Welling, M. (2014). Auto-encoding variational bayes.
- Krizhevsky, A., Sutskever, I., and Hinton, G. E. (2012). Imagenet classification with deep convolutional neural networks. In Pereira, F., Burges, C. J. C., Bottou, L., and Weinberger, K. Q., editors, *Advances in Neural Information Processing Systems*, volume 25. Curran Associates, Inc.
- Krizhevsky, A., Sutskever, I., and Hinton, G. E. (2017). Imagenet classification with deep convolutional neural networks. *Communications of the ACM*, 60:84–90.
- Leontiadis, I., Laskaridis, S., Venieris, S. I., and Lane, N. D. (2021). It’s always personal: Using early exits for efficient on-device cnn personalisation. In *Proceedings of the 22nd International Workshop on Mobile Computing Systems and Applications*, HotMobile ’21, page 15–21, New York, NY, USA. Association for Computing Machinery.
- Molchanov, P., Mallya, A., Tyree, S., Frosio, I., and Kautz, J. (2019). Importance estimation for neural network pruning. In *IEEE Conference on Computer Vision and Pattern Recognition, CVPR 2019, Long Beach, CA, USA, June 16-20, 2019*, pages 11264–11272. Computer Vision Foundation / IEEE.
- Rajagopal, A. and Bouganis, C. (2021). perf4sight: A toolflow to model CNN training performance on edge gpus. *CoRR*, abs/2108.05580.
- Rajagopal, A. and Bouganis, C.-S. (2020). Now that i can see, i can improve: Enabling data-driven finetuning of cnns on the edge. In *Proceedings of the IEEE/CVF Conference on Computer Vision and Pattern Recognition (CVPR) Workshops*.
- Saenko, K., Kulis, B., Fritz, M., and Darrell, T. (2010). Adapting visual category models to new domains. In Daniilidis, K., Maragos, P., and Paragios, N., editors, *Computer Vision – ECCV 2010*, pages 213–226, Berlin, Heidelberg. Springer Berlin Heidelberg.
- Sandler, M., Howard, A., Zhu, M., Zhmoginov, A., and Chen, L.-C. (2018). Mobilenetv2: Inverted residuals and linear bottlenecks. *Proceedings of the IEEE Computer Society Conference on Computer Vision and Pattern Recognition*, pages 4510–4520.
- Simonyan, K. and Zisserman, A. (2015). Very deep convolutional networks for large-scale image recognition. In Bengio, Y. and LeCun, Y., editors, *3rd International Conference on Learning Representations, ICLR 2015*,

*San Diego, CA, USA, May 7-9, 2015, Conference Track Proceedings.*

Sohn, K., Lee, H., and Yan, X. (2015). Learning structured output representation using deep conditional generative models. In Cortes, C., Lawrence, N., Lee, D., Sugiyama, M., and Garnett, R., editors, *Advances in Neural Information Processing Systems*, volume 28. Curran Associates, Inc.

Zhang, J., Ding, Z., Li, W., and Ogunbona, P. (2018). Importance weighted adversarial nets for partial domain adaptation. *CoRR*, abs/1803.09210.

## A. Hyperparameters

### A.1. VAE Training Hyperparameters

As described in (Bowman et al., 2015), the value of  $\beta$  changes over the course of training and is initialised at 0 (favouring reconstruction only) and gradually increased in steps of  $\delta_\beta$  every  $ep_\beta$  epochs of training. Furthermore, the training process has the hyperparameters of  $bs^{vae}$  (training batch size),  $lr_0^{vae}$  (initial learning rate),  $\gamma^{vae}$  (learning rate multiplier),  $ep_{lr}^{vae}$  (learning rate step size).

#### A.1.1. TRAINING HYPERPARAMETERS

For all experiments in the following sections unless mentioned otherwise, the following values are used for the introduced hyperparameters:

- $|z| = 16$  (size of the latent space),  $s = 1000$  (number of classes in ILSVRC'12)
- $q_\phi(z|\mathcal{A}_s, y_s)$  is estimated using a four layer fully connected neural network with layer sizes  $[|\mathcal{A}_s| + s, 1024], [1024, 128], [128, 64], [64, |z|]$  with ReLU non-linearities.
- $p_\theta(\mathcal{A}_s|z, y_s)$  is estimated using a two layer fully connected neural network with layer sizes  $[|z| + s, 512], [512, |\mathcal{A}_s|]$  with ReLU non-linearities.
- Adam (Kingma and Ba, 2015) optimiser with  $bs^{vae} = 512$ ,  $lr_0^{vae} = 1e^{-3}$ ,  $\gamma^{vae} = 0.1$ ,  $ep_{lr}^{vae} = 30$  - This is set such that the learning rate only changes after the value of  $\beta$  has reached 1.
- 90 epochs of training are performed in total.

### A.2. Retraining Hyperparameters

- $R = 3000$
- Stochastic Gradient Descent (SGD) optimiser with 50 epochs of retraining, batch size 32, initial learning rate of  $1e^{-6}$ , learning rate changes every 15 epochs with  $\gamma = 0.1$ , momentum of 0.9 and no weight decay.

### A.3. On-device Retraining Hyperparameters

For the TFO and OFA methodologies, 10 epochs of retraining are performed with an initial learning rate of  $1e^{-3}$  which is decayed by 0.1 every 3 epochs. For PersEPhonEE, as discussed in (Leontiadis et al., 2021), 10 epochs of retraining are performed with an initial learning rate of  $1e^{-2}$  that is left unchanged.

## B. Further Experiments

This section discusses additional experiments performed to identify the limits of LoCO-PDA.

	$\mathcal{M}_{TFO}^0$ (%)					
	NO UNCERTAINTY			UNCERTAINTY		
	NO RETRAIN	NO RETRAIN	RETRAINED	LoCO-PDA	RETRAINED	LoCO-PDA
CITY (185)	74.44	65.72	68.80	69.70	60.45	68.09
MOTORWAY (26)	72.03	63.87	71.51	72.55	57.91	69.34
COUNTRY-SIDE (204)	74.96	66.61	69.18	70.35	63.57	69.30
OFF-ROAD (26)	78.85	70.73	85.78	86.19	77.30	82.27

Table 7. On-device domain adaptation accuracy of a 50% pruned MobileNetV2 network. The table titles are the same as in Table.4.

### B.1. Other network architectures

#### B.1.1. MOBILENETV2 (SANDLER ET AL., 2018)

The results from Sec.6 demonstrate that LoCO-PDA generalises well across different pruning strategies (TFO, OFA) for the same backbone network (ResNet50). This section evaluates LoCO-PDA’s generalisability to other networks by evaluating it on MobileNetV2. Table.7 displays the accuracy regained by performing on-device memory bounded, classifier-only training and LoCO-PDA on the four autonomous driving  $\mathcal{D}'$ .  $\mathcal{M}_{TFO}^0$  is an unpruned MobileNetV2 with 312.3 MFLOPs of inference cost and 14.09 MB of model memory.  $\mathcal{M}_{TFO}^{50}$  is a 50% TFO pruned MobileNetV2 network with 166.6 MFLOPs of inference cost and 7.06 MB of model memory.

Across all  $\mathcal{D}'$ , LoCO-PDA performs 0.88pp better than memory bounded classifier-only retraining. However, although the image based retraining methodology degrades accuracy by 9.01pp in the label uncertain setting compared to label certain setting, LoCO-PDA also degrades accuracy by 2.45pp. This could be due to the lower accuracy of the unpruned MobileNetV2 compared to the networks in Sec.6, thus demonstrating the sensitivity of LoCO-PDA to an overly noisy estimation of  $\mathcal{D}'$ .

#### B.1.2. VGG11 (SIMONYAN AND ZISSERMAN, 2015)

All the networks evaluated thus far and all modern CNN architectures have linear classifiers while AlexNet (Krizhevsky et al., 2012) and VGG11 (Simonyan and Zisserman, 2015) have non-linear classifiers. Consequently, utilising a CVAE, with significantly lower expressive power than a feature extractor, to estimate the activations of networks such as AlexNet and VGG is challenging. Furthermore, the dimensionality of the input to VGG11’s feature extractor has 10,388 neurons making it challenging to create a CVAE architecture with a reasonable memory footprint to estimate so many neurons. Preliminary results fail to successfully train small VAEs to estimate the activations of VGG11 and further exploration of this limitation is left for future work.

### B.2. Unconditional vs Conditional VAEs

Instead of training a single CVAE for all 1000 classes of ILSVRC’12, it is possible to train smaller unconditional VAEs per class and depending on the activation desired,

	TOP1 TEST ACCURACY (%)				MEMORY (MB)
	CITY (185)	MOTORWAY (26)	COUNTRY-SIDE (205)	OFF-ROAD (26)	
CONDITIONAL	73.84	76.75	74.03	87.30	10
UNCONDITIONAL	73.92	74.92	74.18	88.02	400

Table 8. Comparison of retraining accuracy and VAE model memory consumption when using a single CVAE vs 1000 unconditional VAEs. The network is an 80% pruned ResNet50.

the appropriate VAE is sampled. The architecture of the VAE used is provided in Appendix C, and each VAE consumes only 0.4 MB. This experiment explores if conditioning the VAE on classes causes any loss in representation capabilities. Table.8 shows the results for no label space uncertainty retraining of  $\mathcal{M}_{TFO}^{80}$  for various  $\mathcal{D}'$  using LoCO-PDA. The results demonstrate that on average across  $\mathcal{D}'$ , the unconditional approach performs 0.22pp worse than one CVAE while consuming 40x more memory. Thus, a conditional architecture has significant memory benefits and similar representation capabilities as the unconditional architecture.

## C. Architectures, Hyperparameters

For all experiments other than those in Appendix B.2, the VAE architecture described in Appendix A.1 is used. For the experiment in Appendix B.2, the CVAE follows this same architecture however the architecture of the VAE is as follows:

- $m = 2, s = 1000$  (number of classes in ILSVRC’12)
- $\mathcal{A}_q$  is a three layer fully connected neural network with layer sizes  $[n + s, 128], [128, 64], [64, m]$  with ReLU non-linearities.
- $\mathcal{A}_p$  is a two layer fully connected neural network with layer sizes  $[m + s, 64], [64, n]$  with ReLU non-linearities.

For all experiments other than those in Sec.6.7, the LoCO-PDA hyperparameters provided in Appendix A.1 were used. For the results provided in Sec.6.7, training schedule followed as as follows:

- SGD optimiser with 5 epochs of retraining, batch size 32, initial learning rate  $1e^{-6}$ , with no learning rate changes, momentum of 0.9 and no weight decay.

## D. Target Domain Datasets ( $\mathcal{D}'$ )

This section provides details on the classes present in all the source and target domains discussed in Sec.6. The details of the classes present in the four autonomous driving  $\mathcal{D}'$  are:

- **City** (185 classes) : ambulance, trash can, station wagon, tandem bike, taxi, car mirror, car wheel, con-

vertible, crane, electric locomotive, fire engine, fire truck, garbage truck, petrol pump, radiator grille, jeep landrover, rickshaw, lawn mower, limousine, mailbox, manhole cover, minibus, minivan, Model T, moped, scooter, mountain bike, moving van, parking meter, passenger car / coach, pay-phone, pickup truck, police car, race car, school bus, shopping cart, snowplow, sports car, steel arch bridge, tram, suspension bridge, tow truck, trolley bus, street sign, traffic light, palace, mosque, church building, castle, boathouse, triumphal arch, academic gown/robe, cardigan, fur coat, gown, jersey / t-shirt, suit, sunglasses, sweatshirt, trench coat, umbrella, swan, dogs, red fox, cats

- **Motorway** (26 classes) : station wagon, bullet train, car mirror, car wheel, convertible, electric locomotive, petrol pump, jeep landrover, minibus, minivan, mobile home, Model T, moving van, passenger car / coach, pay-phone, pickup truck, police car, race car, recreational vehicle, snowplow, sports car, tow truck, trailer truck, street sign, water tower
- **Country-side** (204 classes) : wheelbarrow, station wagon, bullet train, taxi, car mirror, car wheel, convertible, electric locomotive, freight car, garbage truck, petrol pump, radiator grille, half track, horse cart, jeep landrover, lawn mower, mailbox, manhole cover, minibus, minivan, mobile home, Model T, moped, scooter, mountain bike, moving van, oxcart, parking meter, passenger car / coach, pay-phone, picket-fence, pickup truck, plough, police car, race car, recreational vehicle, school bus, snowmobile, snowplow, sports car, steel arch bridge, tank, thatched roof, tile roof, tow truck, tractor, trailer truck, worm fence, street sign, traffic light, hay, palace, mosque, church building, castle, lighthouse, barn, viaduct, water tower, cardigan, fur coat, gown, sarong, jersey / t-shirt, suit, sunglasses, sweatshirt, swimming trunks, trench coat, umbrella, cock, hen, quail, goose, swan, dogs, red fox, cats, rabbits, ram, sheep
- **Off-road** (26 classes) : mobile home, mountain bike, oxcart, pickup truck, plough, snowmobile, tank, tractor, hay, ostrich, iguana, alligator, wallaby, koala, wombat, brown bear, black bear, hog, wild boar, ox, water buffalo, bison, wild deer

- back\_pack, bike, calculator, headphones, keyboard, laptop\_computer, monitor, mouse, mug, projector

There are fewer written categories than the number of classes stated as some categories such as "dogs" have many ILSVRC'12 classes within them. There is also overlap of classes between the subsets as would be expected. For the Office-31 dataset, the 10 classes (which are the same for each of the 3 categories of images) that made up the various  $\mathcal{D}'$  are:

# Number of Accepted Papers

